THE EFFECT OF PRIME MOVER REGENERATOR RADIUS ON THE PERFORMANCE AND CHARACTERISTIC OF ACOUSTIC FIELD OF THERMOACOUSTIC REFRIGERATOR DRIVEN BY PRIME MOVER

Irna FARIKHAH[1*], Rifqi Nurfadhilah ISNANDI[1], Ikhsan SETIAWAN[2], Rifki HERMANA[1], Endang Dian ROKHMAWATI[3], Harto NUROSO[4], Mega NOVITA[5], Margono[6]

[*1] Department of Mechanical Engineering, Universitas PGRI Semarang, Indonesia

[2]Department of Physics, Universitas Gadjah Mada, Indonesia

[3]Department of Physics Education, Universitas Negeri Semarang, Indonesia

[4]Department of Physics Education, Universitas PGRI Semarang, Indonesia

[5]Graduate School of Natural Science Education, Universitas PGRI Semarang, Indonesia

[6]Department of Electrical Engineering, Universitas PGRI Semarang, Indonesia

[*]Corresponding author; E-mail: irnafarikhah@upgris.ac.id

Abstract

Refrigerated truck is indispensable transportation for food and medicine. However, the truck has been using the harmful substance such as CFC or HCFC. Therefore, an alternative cooler is essential such as thermoacoustic refrigerator. The refrigerator is driven by the thermoacoustic heat engine (prime mover), so the prime mover can convert the thermal or waste heat into the acoustic energy for driving the refrigerator. There are some parameters that can improve the efficiency of the refrigerator system. The aim is to investigate the impact of prime mover regenerator radius on the efficiency and characteristic of acoustic field. It was found that the best performance of the whole refrigeration system was achieved when the radius is 0.68. The engine and cooler efficiency are 84 % and 38 %, respectively. In addition, the acoustic field characteristic was also analyzed to elucidate the mechanism in the refrigerator system.

Keywords: prime mover; refrigerator

1. Introduction (Word Style TS Heading)

Semi-trailer insulated rigid boxes is the common refrigerated road transportation for foods [1]. Refrigeration in the boxes is essential to maintain the cooling temperature to keep fresh the food. The refrigeration process in the trailer is fueled by the diesel engine which contributes to the green-house gas emission, so it is important to handle the issue. Moreover, the diesel engine is part of non-renewable energy. Therefore, the use of renewable energy is indispensable for the global sustainable energy [2]. The sector of energy has been changed in good approachs to the acceptance of various green energy and innovation. Report from Global Renewable Outlook: Energy Transformation 2050, green energy and its performance together over 90 % of the mitigation measures needed to decrease power-related emissions [3]. Increased use of the refrigeration system is one of the reasons of high greenhouse emissions nowadays [4]. To achieve this transforming energy-related emissions scenario,

converting a low-grade waste heat energy into refrigeration technology is such a good move to try. Several studies related unused heat recovery technology have been done, for organic rankine cycle [5], turbo compounding [6], and thermoacoustics technology [7]. Thermoacoustic is one of the best methods to recover the low-grade waste heat, as it have a uncomplicated construction [7], motionless [8] and environment friendliness [8]. Thermoacoustic is type of energy-regeneration innovation which can be used for heating and refrigeration [9-11] or power generation [12]. A heat-driven thermoacoustic refrigerator is a new sort of feasible heat-driven refrigeration innovation that comprises of a prime mover and a thermoacoustic refrigerator. It converts heat into sound energy to transport heat from lower to higher temperatures using regenerator [13].

Thermoacoustic engines composed of a regenerator (REG), an ambient heat exchanger (AHX), a hot heat exchanger (HHX) and a thermal buffer tube (TBT) and a tube [12, 14]. As the initial temperature difference at two edges of the regenerator surpass a certain value, spontaneous gas oscillation occurs and produced acoustic power [15], so for the utilization of low temperature, it is important to decrease the required initial temperature in the prime mover. Some investigations have been conducted to enhance the prime mover performance. Based on Swift and Backhaust, the use of looped pipe has higher performance than using straight pipes [16]. The reason is the circle pipe is moved by a traveling wave that performs operations with a reversible Stirling cycle compared to a straight pipe that is conducted by a standing wave so that it undergoes an irreversible process [17]. Travelling wave thermoacoustic engine was investigated by Utami, Rahmawati and Farikhah. They studied the impact of geometry on the prime mover efficiency [9,14,18]. The prime mover can drive the thermoacoustic refrigerator. Farikhah et.al investigated the effect of some geometry parameters in the heat driven thermoacoustic refrigerator [19, 20, 21].

There are some studies about the effect of regenerator radius. Utami et. al [14] and Yang [21] studied the influence of stack radius, but these were only for the performance of prime mover not for a combination of prime mover and refrigerator. In 2017, Farikhah and Ueda studied about the effect of regenerator radius on the efficiency of a heat driven thermoacoustic cooler. However, the setting cooling temperature was extremely low at about 251 K and it was lack of elucidation of the acoustic field characterization and mechanism. It was found that the optimum regenerator radius is 1 [20]. We consider that the optimum radius would be shift when the cooling temperature is set at 273 K. Therefore, the effect of the radius on the performance of the thermoacoustic refrigerator driven by the prime mover and the characteristic of the acoustic field is investigated for cooling temperature 273 K.

2. Method

2.1. Calculation Model

The Model of the refrigeration system is shown in Fig. 1. It comprises of some components; ambient heat exchanger, regenerator of prime mover, hot heat exchangers, thermal buffer tubes, cold heat exchanger and the cooler regenerator which installed inside the looped tube. The detail values and the gas properties are provided at table 1 and 2. The working gas is helium at 3 MPa. In this calculation, the beginning heating temperature in the prime mover T_h is one of the calculation results while the cooling temperature T_c is set at 273 K. In this calculation, we did not take into account the value of thermal conductivity of the regenerator because we assumed that the material of regenerators has very low thermal conductivity such as mylar, so the heat which has been pumped by the refrigeration system will not be conducted back to the cold side for the refrigerator. For heat exchanger, we assumed that the heat exchanger has high thermal conductivity such as copper, so the heat transfer works well.

The heating temperature of the hot heat exchanger is denoted as T_h and T_a is the ambient temperature in the ambient side of the exchanger, while T_c is the cooling temperature of the cold exchanger. In this calculation, T_h is one of the result of stability limit calculation [20], whereas T_a and T_c are 301 K and 273 K, respectively.

Table 1. The Specifications

Geometrical Parameters	Value		
	Length (mm)	Radius (mm)	Porosity (-)
Looped tube	2800	20	-
Heat exchangers	10	0.5	0.5
Prime mover Regenerator	40	0.05 – 0.15	0.77
Thermal buffer tubes	600	20	-
Refrigerator Regenerator	40	0.5	0.77

Table 2 The Gas Properties

The properties	Value
P_m	3 MPa
γ	1.6632
ρ_m	4.749 kg/m^3
σ	0.6579
χ_α	0.8594
χ_v	0.7608

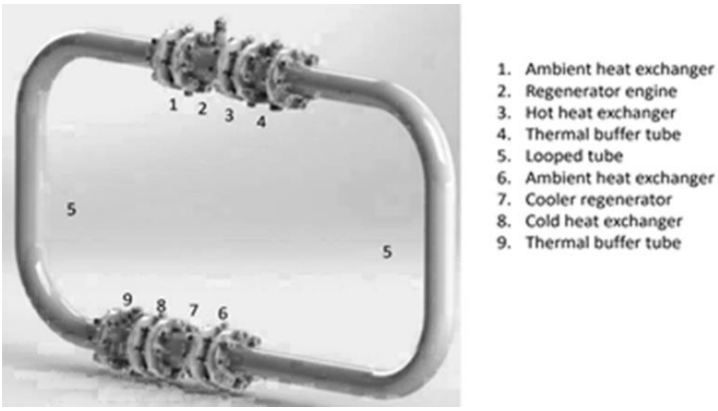

Figure. 1. The Thermoacoustic Refrigerator driven by a Prime Mover

2.2. Numerical Calculation

For the computational calculation, we used Rott's thermoacoustic concept and the transfer matrix method for oscillatory pressure P and volume velocity U. Using acoustic approximation of Rott [10], the equation of momentum and continuity are presented as:

$$\frac{dP_1}{dx} = -\frac{i\omega\rho_m}{1-\chi_v} U_1 \qquad 1)$$

$$\frac{dU_1}{dx} = -\frac{i\omega[1+(\gamma-1)\chi_\alpha]}{\gamma P_m} P_1 + \frac{\chi_\alpha - \chi_v}{(1-\chi_v)(1-\sigma)} \frac{1}{T_m} \frac{dT_m}{dx} U_1 \quad 2)$$

Where P is the oscillation pressure, U as the velocity, ω is the angular frequency of the acoustic wave, A is the cross-sectional area of the channel, and ρ_m, P_m, γ, and σ are the mean density, mean pressure, ratio of specific heats, Prandtl number of the working gas. Additionally, χ_α and χ_v constitutes the thermoacoustic functions that depend on the proportion of the radius r of the narrow channel(s) and the penetration depth. The value of dT_m/dx is expressed as follows:

$$\frac{dT_m}{dx} = \frac{(\dot{W} - \dot{Q}) - \frac{A}{2} Re\left[P\tilde{U}\left(1 - \frac{\tilde{\chi}_v - \chi_\alpha}{(1+\sigma)(1-\tilde{\chi}_v)}\right)\right]}{\frac{A\rho_m c_p |U|^2}{2\omega(1-\sigma^2)|1-\chi_v|^2} Im[\chi_\alpha + \sigma\tilde{\chi}_v]} \quad (3)$$

In order to find the performance of thermoacousctic's refrigerator system, we can use transfer matrix from Eq. (1) and Eq. (2) presented as below:

$$\frac{d}{dx}\begin{pmatrix} P_1(x,t) \\ U_1(x,t) \end{pmatrix} = B(x)\begin{pmatrix} P_1(x,t) \\ U_1(x,t) \end{pmatrix} \quad 4)$$

$$B(x) \equiv \begin{pmatrix} 0 & \frac{-i\omega\rho_m}{(1-\chi_v)} \\ \frac{-i\omega[1+(\gamma-1)\chi_\alpha]}{\gamma P_m} & \frac{\chi_\alpha - \chi_v}{(1-\chi_v)(1-\gamma)} \frac{1}{T_m} \frac{dT_m}{dx} \end{pmatrix}$$

From above matrix, we can understand that $\rho_m, \gamma, \chi_v, \chi_a$, and σ depend on T_m, i.e., on x. So, the Eq. (4) can be solved empirically if dTm/dx=0. When $dTm/dx \neq$0, it's hard to solve the Eq. (4) analytically. We can calculate it by mathematically integrated by employing a forward difference scheme utilizing the fourth-order Runge-Kutta method to Eq. (4).

$$\begin{pmatrix} P_1(x+\Delta x,t) \\ U_1(x+\Delta x,t) \end{pmatrix} = \big(D + \Delta x B'(x)\big)\begin{pmatrix} P_1(x) \\ U_1(x) \end{pmatrix} \quad 5)$$

$$B'(x) = (1/6)(RK_1 + 2RK_2 + 2RK_3 + RK_4)$$

$$RK_1 = B(x)$$

$$RK_2 = B\left(x + \frac{\Delta x}{2}\right)\left(D + \frac{\Delta x}{2} RK_1\right)$$

$$RK_3 = B(x + \Delta x/2)(D + (\Delta x/2)RK_2)$$

$$RK_4 = B(x + \Delta x)(D + \Delta x RK_3)$$

Where D is a unit matrix, the value of P and U can be calculated by:

$$\begin{pmatrix} P_1(x,t) \\ U_1(x,t) \end{pmatrix} = M_{II}(x, x_0)\begin{pmatrix} P_0(x_0,t) \\ U_0(x_0,t) \end{pmatrix} \quad 6)$$

$$M_{II}(x, x_0) \equiv (D + \Delta x B'_{n-1})(D + \Delta x B'_{n-2}) \ldots (D + \Delta x B'_1)(D + \Delta x B'_0)$$

When P and U are provided at one position, the distributions of P and U can be calculated.

The Eq. (6) can be used to compute the transfer matrix both in prime mover regenerator $M_{11,es}$ and refrigerator regenerator $M_{11,cs}$. The whole movement-track areas in the parts are different from each other, so the join matrix is as follows:

$$Y_{d,e} = \begin{pmatrix} 1 & 0 \\ 0 & A_d/A_e \end{pmatrix} \quad (7)$$

The total area and the component number are denoted by *A*, *d* and *e*, respectively. The transfer matrices components and join matrices are used to convey the transfer matrix of the entire system as:

$$M_{tot} = M_{10}O_{10,9}M_9O_{9,8}M_8O_{8,7}M_7O_{7,6}M_6O_{6,5}M_5O_{5,4}M_4O_{4,3}M_3O_{3,2}M_2O_{2,1}M_1 \quad (8)$$

By using the Eq. (8), the oscillatory pressure $P_{e,A}$ and cross-sectional mean of oscillatory velocity $U_{e,A}$ are related to the oscillatory pressure $P_{e,B}$ and cross-sectional mean of oscillatory velocity $U_{e,B}$ as

$$M_{tot}\begin{pmatrix} P_{e,A} \\ U_{e,A} \end{pmatrix} = \begin{pmatrix} P_{e,B} \\ U_{e,B} \end{pmatrix} \quad 9)$$

If we got the result of zero from determinant matrix ($M_{tot} - D$), where *D* is the unit matrix, we can use the following equation:

$$(m_{11} - 1)(m_{22} - 1) - m_{12}m_{21s} = 0 \quad (10)$$

When Eq. (10) is numerically solved, the stability limit condition can be reached, than spontaneous gas oscillation can be excited in the prime mover and the initial heating temperature was obtained. In the stability limit, the impedance $Z = P/U$, angular frequency ω and T_h are the results. These results were calculated with transfer matrix by changing the radius of the perime mover regenerator. Then, the entire performance can be found.

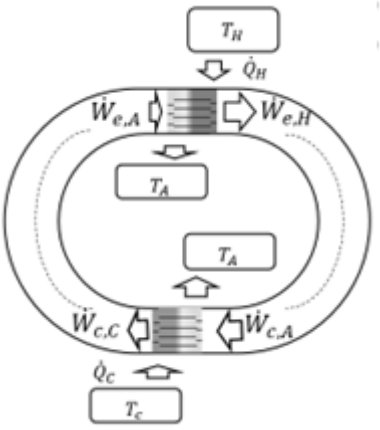

Figure 2. Schematic Illustration and Mechanism of the refrigerator driven by the prime mover.

The schematic illustration of the system is shown in Fig. 2 $\dot{W}$ and $\dot{Q}$ denote the acoustic power and the thermal power, respectively. These values can be expressed as follows:

$$\dot{W} = \frac{A}{2}Re\left[P\tilde{U}\right] \quad 11)$$

$$\dot{Q} = \frac{A}{2}Re\left[P\tilde{U}\left(\frac{\tilde{\chi}_v - \chi_\alpha}{(1+\sigma)(1-\tilde{\chi}_v)}\right)\right] - \frac{A\rho_m c_p|U|^2}{2\omega(1-\sigma^2)|1-\chi_v|^2}\, Im[\chi_\alpha + \sigma\tilde{\chi}_v]\frac{dT_m}{dx} \quad 12)$$

where the axial coordinate along the looped tube is denoted as x and the complex conjugation is expressed as tilde. T_m and c_p denote as mean temperature and specific heat at the constant pressure, respectively.

Fig. 2 shows the schematic illustration and mechanism of the system. $\dot{W}_{e,A}$ is acoustic power at the ambient end of the prime mover regenerator and it is amplified in the regenerator prime mover. The amplified acoustic power is denoted as $\dot{W}_{e,H}$. It is emitted from the hot end of the regenerator prime mover. The acoustic power gain of the regenerator prime mover is denoted as $\Delta\dot{W}_e$ and it can be expressed as as:

$$\Delta\dot{W}_e = \dot{W}_{e,H} - \dot{W}_{e,A} \tag{13}$$

The thermal power $\dot{Q}_H$ is needed to amplify the acoustic power. Therefore, the prime mover efficiency can be expressed as follows:

$$\eta_e = \Delta\dot{W}_e/\dot{Q}_H \tag{14}$$

The acoustic power emitted from the hot end of the prime mover then it travels along the looped tube and dissipates along the looped tube. After that, it enters the ambient side the refrigerator regenerator, $\dot{W}_{c,A}$. The acoustic power is used to pump the heat from the cold side to the ambient side of the refrigerator regenerator. Then, the acoustic power output at the cold heat exchanger, $\dot{W}_{c,C}$ travels and dissipates along the tube and it enters again to the prime mover regenerator. The cooling power is denoted as $\dot{Q}_c$ so that the Coefficient of Performance (*CoP*) is expressed as:

$$CoP = \dot{Q}_c/\left(\dot{W}_{c,A} - \dot{W}_{c,C}\right) \tag{15}$$

The transmission line in the system is the looped tube, so the efficiency of the tube is

$$\eta_{tube} = \left(\dot{W}_{c,A} - \dot{W}_{c,C}\right)/\Delta\dot{W}_e \tag{16}$$

In this calculation, we calculated the second-law efficiency of prime mover regenerator $\eta_{2,e}$. It can be written as follows

$$\eta_{2,e} = \eta_e/\eta_{Carnot} \tag{17}$$

where η_e is the thermal efficiency and η_{Carnot} is the thermodynamic upper limit value of η_e. η_{Carnot} can be calculated as follows:

$$\eta_{Carnot} = (T_H - T_A)/T_H \tag{18}$$

The second-law efficiency of the cooler $\eta_{2,c}$ can be defined as follow:

$$\eta_{2,c} = COP/COP_{Carnot} \tag{19}$$

COP_{Carnot} is the thermodynamic upper limit value of COP. it can be calculated as follows :

$$COP_{Carnot} = T_C/(T_a - T_c) \tag{20}$$

where T_a and T_c are the ambient and cooling temperature, respectively.

To find the total efficiency of the refrigerator system ($\eta_{all,2}$), we can calculate it by:

$$\eta_{all,2} = \eta_{2,e}.\eta_{2,c}.\eta_{tube} \tag{21}$$

2.3. Boundary Conditions

Fortran95 was used for the simulations. The momentum and continuity equations were used to simulate the thermoacoustic refrigerator driven by prime mover. In this calculation, the prime mover

radius was varied to find the best performance. There are two calculations in this simulation. Stability limit and efficiency calculation. For stability limit calculation [20], with changing the radius of the prime mover, we can obtain the heating temperature of the prime mover T_h, impedance P/U and the anguler frequency ω. These results were used for calculating the efficiency. Here, the cooling temperature of the refrigerator was set at 273 K. For better understanding, the boundary condition was shown in Fig. 3. The looped tube was modelled as a straight tube.

The boundary conditions was set as follows:

At $x = 0 = L_{loop}$ and y loop $\begin{cases} P_A/U_A = P_B/U_B \\ V = 0 \end{cases}$

where U, V and P are velocity in the x and y axis and pressure, respectively. As can be seen in Fig. 3, the initial point is at the ambient heat exchanger. At this point, the impedance P/U at A is the same as at B.

At x = Length of regenerator $\begin{cases} \frac{dT}{dx} \neq 0 \\ \frac{dT}{dy} = 0 \end{cases}$

At $x_1 = x_2$ =loop tube $\begin{cases} \frac{dT}{dx} = 0 \\ \frac{dT}{dy} = 0 \end{cases}$

The pressure, velocity and temperature are expressed as in terms of a mean component as follows

$$P = P_m + Re\{P_1 e^{i\omega t}\} \quad (22)$$

$$U = Re\{U_1 e^{i\omega t}\} \quad (23)$$

$$T = T_m + Re\{T_1 e^{i\omega t}\} \quad (24)$$

where T_m is the mean temperature and P_m is the mean pressure. T_1, U_1, and P_1 are the temperature, velocity and the pressure oscillations of the travelling wave and $Re\{\ \}$ is the real part which $e^{i\omega t}$ is the time dependency of a particular variable and ω is the angular frequency. In this study, we assumed that the tube wall heat capacity is higher than that of the working gas. Therefore, we assume that tube-wall temperature is constant and we did not take into account the thermal permeability parameters. Nevertheless, the calculation was already validated with Yazaki's experimental results [22] shown in Fig. 4.

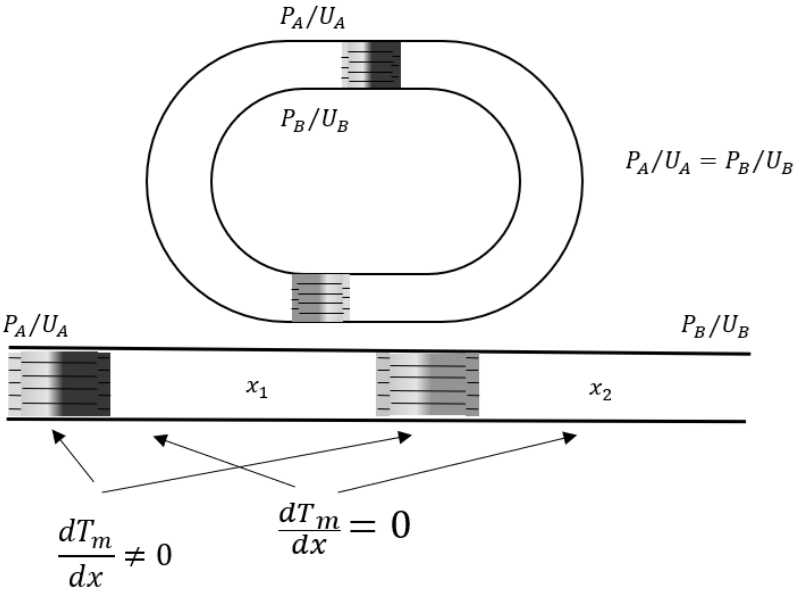

Figure 3. the looped tube as model of straight tube

The temperature gradient along the regenerator with $dT_m/dx \neq 0$ can be calculated by coupling Equations (1) – (3) if the boundary conditions about P_A and U_A are given. However, it is not possible to determine the absolute values of P and U . Nevertheless, the relative values can be obtained with the pressure amplitude at the initial position (at the ambient end of the prime mover) $|P_{e,A}|$ is 6.8 kPa. By using the obtained T_H, P/U, ω and the transfer matrices, the acoustic field distribution along the looped tube can be calculated. As a result,we can calculate the efficiency. It should be noted that the evaluated performance was determined as a dimensionless value, and, thus, the pressure amplitude did not impact the results.

2.4. Validation of the numerical calculation and the experimental result

Fig. 4 shows the validation between the Yazaki's experimental result and the numerical one. As we can see, the pressure amplitude $|P|$, Velocity $|U|$ and the phase different φ have a good agreement between the experimental work and the calculation.

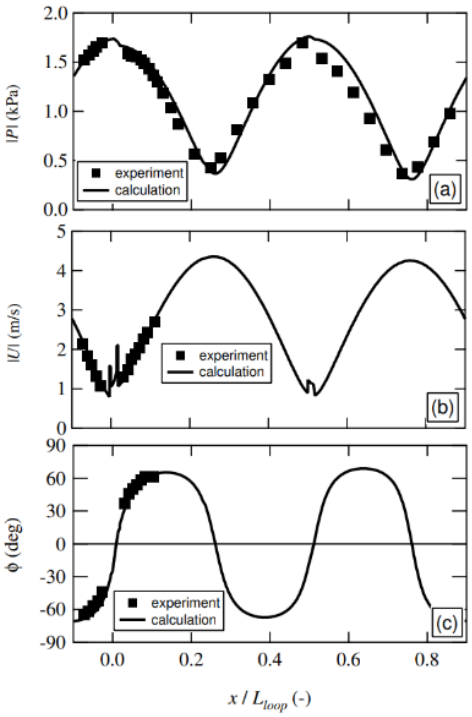

Figure. 4. $|P|$, $|U|$, and φ as a function of x/L_{loop}. The symbols show the experimental results obtained from the article [20, 22].

3. Result and Discussion.

3.1. Efficiency of Thermoacoustic Refrigerator driven by prime mover

Yang et.al reported that there is a dependence of radius of regenerator on the performance of thermoacoustic engine (prime mover) [21]. However, they just focus on the engine. Farikhah and Ueda in 2017 reported that the radius of the prime mover and cooler has an impact on efficiency of the entire cooler system. However, the cooling temperature is extremely low at 251 K [20]. In this investigation, therefore, we investigated the effect of prime mover radius on the performance of the whole refrigeration system at 273 K.

Fig. 5 presents the whole efficiency of the cooler system. The *x*-axis shows the ratio between radius of the engine regenerator r_e to thermal penetration depth δ. The heat penetration depth is defined as the distance that the thermal energy diffuses through the regenerator material. The radius is denoted as r_e/δ. As we can see in Fig. 5, the whole efficiency of the system $\eta_{2,all}$ reaches 6.4 % of the upper limit value when r/δ_e corresponds to 0.68. This result is lower than that of obtained by Farikhah and Ueda [20]. It shift from 1 to 0.68.

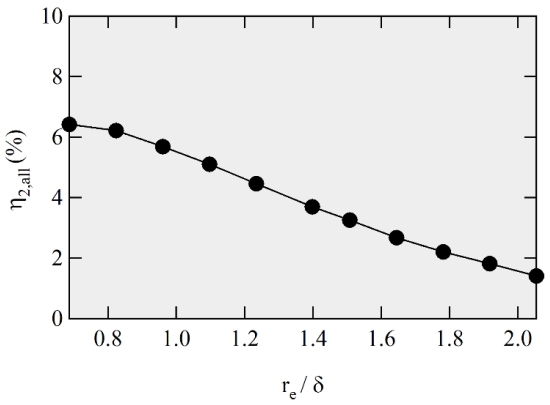

Figure. 5. r_e/δ as a function of $\eta_{2,all}$

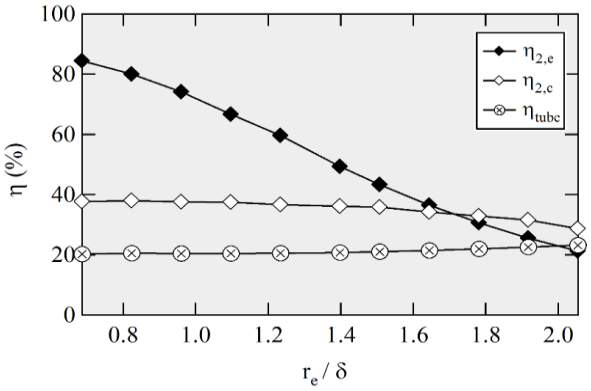

Figure. 6. r_e/δ as a function of $\eta_{2,e}$, $\eta_{2,c}$ and η_{tube}

The entire performance of the refrigerator $\eta_{2,all}$ comprises of second law efficiency of the prime mover $\eta_{2,e}$, tube η_{tube} and the cooler $\eta_{2,c}$. Second law efficiency of the engine $\eta_{2,e}$ is shown in Fig. 6. The prime mover efficiency $\eta_{2,e}$ is superior when r_e/δ is 0.68, and it achieved about 84 % of the carnot efficiency, while the performance of the tube η_{tube} and cooler $\eta_{2,c}$ almost remains constant when the radius is varied. It means that the superior efficiency of system depends on the engine performance. The value of thermal penetration depth is 0.073 mm and the radius is 0.05 mm. According to equation 17, the Second law efficiency engine depends on the value of thermal efficiency η_e and Carnot Efficiency η_{Carnot}. Fig. 7 shows that Carnot efficiency remains constant whereas the thermal efficiency of the prime mover is decreasing from 43 % to about 10 % as the radius is increasing from 0.68 to 2.05.

Since the thermal efficiency η_e of the prime mover is due to the high value of the whole system, so the acoustic power gain $\Delta\dot{W}_e$ and the heating power $\dot{Q}_H$ must be clarified. It is because the thermal performance depends on the ratio of acoustic and heating power [see eq. 14]. As shown in Fig. 8, the thermal power increases from slightly above 0.2 W to about 0.35 W as the engine radius rises from 0.68 to 2.05. On the other hand, the acoustic power gain increases as the radius rises. Based on eq. 14, and the values shown in Fig. 8, the reason of the high value of the thermal efficiency at radius 0.68 is the superior value of acoustic power with low value of heating power.

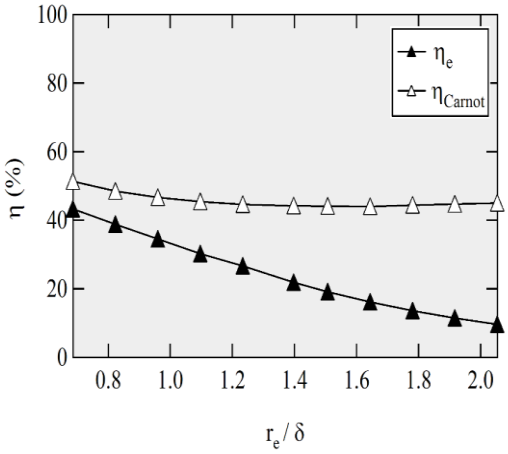

Figure. 7. r_e/δ as a function of η_e and η_{Carnot}

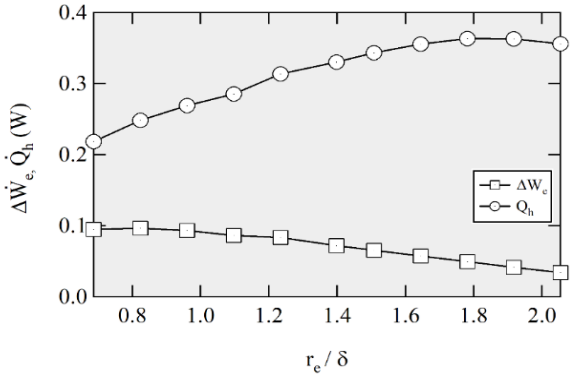

Figure. 8. r_e/δ as a function of η_e and η_{Carnot}

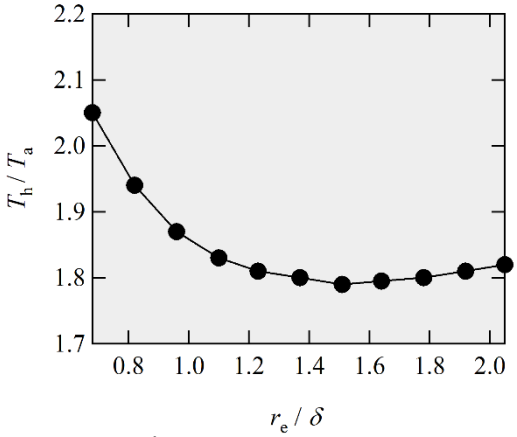

Figure. 9. r_e/δ vs T_h

Fig. 9 shows the heating temperature as a result of simulation. The lowest heating temperature that can be achieved the prime mover is 1.79 which means that the heating temperature $T_h = 538\,K$ and the ambient temperature T_a = 308 K. It was found when the dimensionless radius is 1.51. This heating temperature is lower than that found by Farikhah and Ueda in 2017. They found that the optimum value has 825 K for the heating temperature in the prime mover [20]. We consider that the present results is better for utilizing low-grade waste heat.

3.2. Acoustic Field Characteristic

Fig. 10 shows the the simulation result of the system with r/δ = 0.68. Fig. 10. a. presents the distribution of pressure amplitude P along the looped tube in one wave length which comprises of two troughs and peaks which is the same as that of reported by Jin et.al [23]. Fig. 10.a shows that there are maximum and minimum values of pressure amplitude. It indicates that this is combination between the travelling wave and standing wave. When the ratio maximum and the minimum pressure P_{max}/P_{min} is unity, it means the travelling wave like field. In other words when P_{max}/P_{min} is 1 it is more about travelling wave but if P_{max}/P_{min} far from 1 it means that is more about standing wave [20]. The prime mover and the refrigerator regenerator are put along 0.04 m and 1.17 m, respectively. In this case, both prime mover and refrigerator regenerators are located at the pressure amplitude peak where the acoustic impedance is high. Hence, the performance becomes high. It is the same compare to that of Jin's prime mover location [23], but Jin's refrigerator regenerator was located far away from the peak of the pressure amplitude.

Fig. 10.b. shows the velocity amplitude U. This figure shows the velocity amplitude between the connection of the second wave guide to the ambient heat exchanger. The working gas we used along the looped is Helium which means that the density is the same. However, the total cross-sectional area of the wave guide which is part of the looped pipe is wider than that of hot heat exchanger. As a result, the velocity amplitude in the hot heat exchanger rises. Then, when the velocity enters to regenerator, it decreases. After that, when it is enters the hot heat exchanger, the velocity is rises again. These because of the mass flow rate. The location is the connection between hot heat exchanger and prime mover regenerator. As we can see, the location of prime mover and refrigerator regenerators are at near velocity node which means that the low velocity and viscous loss. Hence, it can decrease one of the sources of inefficiency in the system [24].

Fig. 10.c presents the phase difference (ϕ). As we can see, the phase difference in the hot side and cold side of prime mover regenerators are -39 °and -83 °, respectively. In some cases, negative phase difference ϕ has a good impact on the high value of gain acoustic power of the prime mover $\Delta\dot{W}_e$ as reported by Ueda et.al [25]. The similar result was found in this investigation, as can be seen in Fig. 8, when r/δ *is* 0.68 $\Delta\dot{W}_e$ is the highest one. Ueda et.al reported that negative ϕ is important for producing a large $\Delta\dot{W}_e$ while maintain low viscous loss in the regenerator [25].

Fig. 10.d shows the distribution of acoustic power along the tube. The acoustic power in the hot side of the prime mover is 0.2 W and 0.1 W is the acoustic power in the cold side of the refrigerator. In the prime mover regenerator, the thermal energy is converted into the acoustic energy. Therefore, the acoustic power in the prime mover elevates to 0.2 W. However, in the refrigerator regenerator, the acoustic power drops to 0.1 W. This is because the acoustic power in the refrigerator regenerator is consumed by the regenerator to pump heat from the cold to the ambient side. Thus, the energy conversion between acoustic and thermal energy occurs.

Fig. 10.e shows the impedance of the hot side of the prime mover and the cold side of the refrigerator. The impedances in the engine and cooler are 14.4 and 2.5. The impedance in the prime mover regenerator is much higher than that in the refrigerator regenerator. It has correlation with the efficiency of the prime mover $\eta_{2,e}$ and refrigerator $\eta_{2,c}$ shown in Fig 6. The prime mover efficiency achieves 84 %, but the refrigerator efficiency attains 38 % of the upper limit value.

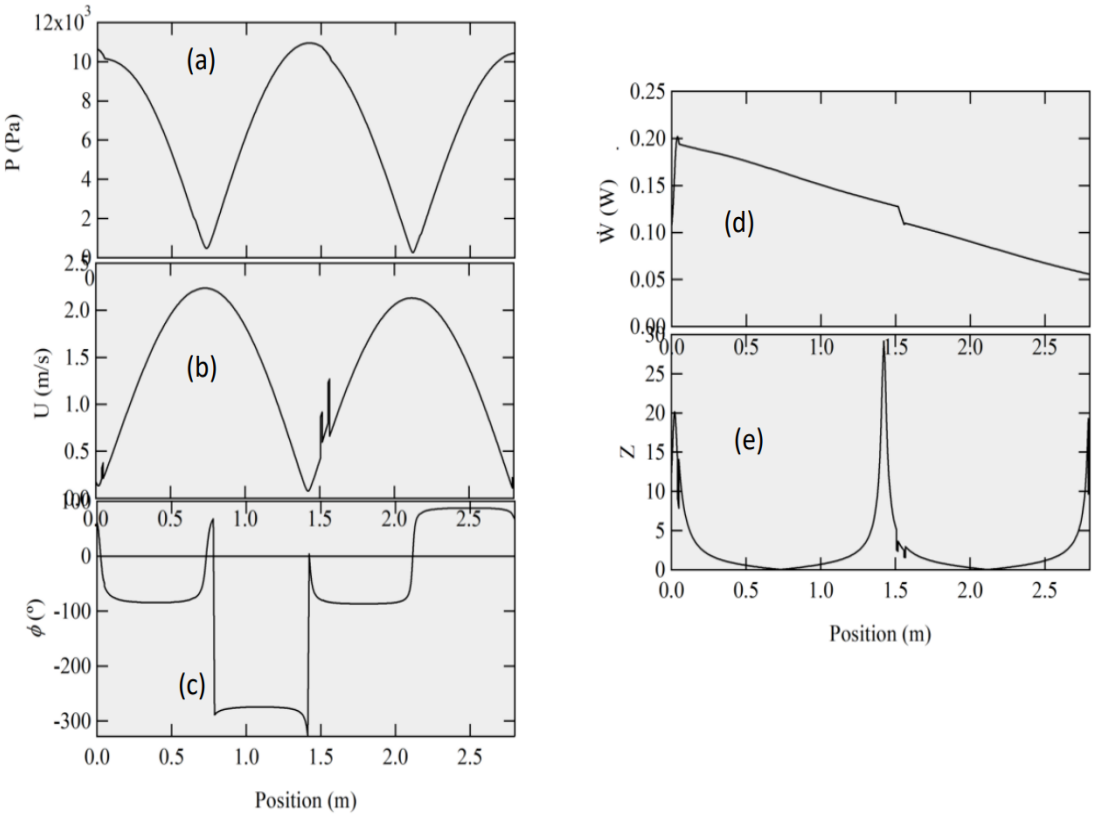

Figure. 10. (a) *P*, (b) *U*, (c) ϕ vs Loop Position

4. Conclusion

In this study, the impact of the regenerator radius on the performance of thermoacoustic refrigerator driven by prime mover was numerically investigated at 273 K of cooling temperature. The investigation has been conducted to analyze the system performance, which can be concluded as follows:

1) It was found that when the dimensionless radius is 0.68, the highest entire system efficiency can be achieved (6.4 %). This efficiency can be divided into three efficiencies; prime mover (84 %), cooler (38 %) and tube (20 %) efficiencies. It can be seen clearly that the prime mover efficiency has high impact on it.
2) By changing the radius ratio of the prime mover regenerator, the acoustic field distributions can be changed for improving the performance. The analysis on the performance at various dimensionless radius, from the perspective of acoustic field distribution / characteristics, indicates that the negative phase difference, large value of acoustic impedance, and low viscous lossess lead to increase the acoustic power gain. Hence, the prime mover efficiency becomes high.
3) The lowest engine heating temperature is 538 K when the dimensionless radius is 1.51.
4) It means that if we focus on how to find high efficiency, the best of the prime mover radius ratio is 0.68, but if we want to utilize the low heating temperature for waste heat recovery, 1.51 is best. These results are guidance for experimental researchers to choose the best ratio of prime mover radius for the refrigeration sytem at 273 K.

5. Acknowledgement

The research work was funded by Ministry of Research and Technology Indonesia through Universitas PGRI Semarang.

6. References

[1] Marshall, R., *et.al*, (Cambridge Refrigeration Technology), *Energy Usage During Refrigerated Transport,* Technical Document prepared for the School of Engineering and Design, Brunel University, July 2006.

[2] Tassou, S. A., *et.al., Food transport refrigeration – Approaches to reduce energy consumption and environmental impacts of road transport*, Applied Thermal Engineering, 29 (2009) 1467-1477.

[3] Gielen, D., *et.al*., *Global Renewables Outlook: Energy Transformation* 2050, International Renewable Energy Agency, Abu dhabi, UEA, 2020.

[4] Dong, Y,. *et.al*, Greenhouse Gas Emissions from Air Conditioning and Refrigeration Service Expansion in Developing Countries, *Annu. Rev. Environtment Resour.*, 46 (2021), pp. 59–83.

[5] Sprous, C., and C. Depcik, Review of organic Rankine cycles for internal combustion engine exhaust waste heat recovery, *Appl. Therm. Eng.*, 51 (2013), pp. 711–722.

[6] Aghaali, H., and Ångström, H, E., A review of turbocompounding as a waste heat recovery system for internal combustion engines, *Renew. Sustain. Energy*, 49 (2015), pp. 813–824.

[7] Zhou, J., M. *et. al*, Study of Thermoacoustic Engine for Automotive Exhaust Waste Heat Recovery, *SAE Technical paper series*, (2019), pp. 1-13.

[8] Jin, T., Application of thermoacoustic effect to refrigeration, *Rev. Sci. Instrum.*,74 (2003). pp. 677-679.

[9] Rokhmawati, E.D., *et. al*, Numerical study on the effect of mean pressure and loop's radius to the onset temperature and efficiency of travelling wave thermoacoustic engine", *AutomotiveExperiences, 103* (2020), 2. pp. 96-103.

[10] Farikhah, I., *et. al*, Numerical Study on the Effect of Stack Radii on the Low Onset Heating Temperature and Efficiency of 4-Stage Thermoacoustic Engine, *Arab. J. Sci. Eng.*, (2022). pp. 1-10.

[11] Farikhah, I., *et.al.*, Thermoacoustic design using stem of goose down stack, *Proceedings,* American Institute of Physics (AIP), 19th International Symposium on Nonlinier Acoustic (ISNA 19). 1474, 2012, pp. 283-286.

[12] Chen, G., *et. al.*, Modelling and analysis of a thermoacousticpiezoelectric energy harvester, *Appl. Therm. Eng.*,*150* (2019),pp. 532–544.

[13] Ueda, Y., and Farikhah, I., Calculation of energy conversion efficiency of a stack-screen Stack using thermoacoustic theory, *TEION KOGAKU (Journal of Cryogenics and Superconductivity Society of Japan), 51* (2016) pp. 403-408.

[14] Utami, S. W., *et. al*., Numerical study of the influence of radius stack on the low heating temperature and efficiency of traveling wave thermoacoustic engine, The 1st International Conference on Education and Technology (ICETECH) 2019, IOP Conf. Series: Journal of Physics: Conf. Series, Madiun, Indonesia, 2020., vol.1, pp. 1-6.

[15] Ueda, Y., Kato, C., Stability analysis of thermally induced spontaneous gas oscillations in straight and looped tubes, *J. Acoust. Soc. Am*., *124* (2008), pp. 851–858.

[16] Backhauss, S., and Swift, G., A thermoacoustic Stirling Engine: Detailed Study, *J. Acoust. Soc. Am.*, *107* (2000), pp. 3149-3150

[17] Yazaki, T., *et. al*., Travelling wave thermoacoustic engine in a looped tube, *Phys. Rev. Lett.*, *81* (1988), pp. 3128–3131.

[18] Farikhah, I., *et. al*., Study of stack length on efficiency of thermoacoustic engine, In *Proceedings* of the 3rd IEEE Eurasia conference on IOT, communication and engineering 2021, Yunlin, Taiwan, 2021, pp. 580-582.

[19] Farikhah, I., and Ueda, Y., The effect of the porosity of stacks on the performance of a heat-driven thermoacoustic cooler, *Proceeding* of the 24th International Conference on Sound and Vibration (24 ICSV) London, 2017, pp. 1-8.

[20] Farikhah, I., Ueda, Y., Numerical calculation of the performance of a thermoacoustic system with engine and cooler regenerators in a looped tube, *Appl. Sci*, *7* (2017), pp. 1-14

[21] Yang, R., *et. al.*, Performance optimization of the regenerator of a looped thermoacoustic engine powered by low-grade heat. *Int J Energy Res*. (2018), pp. 4470– 4480.

[22] Yazaki, T., *et. al*, A. A piston-less Stirling cooler, *Appl. Phys. Lett.*, *80* (2002), pp. 157–159

[23] Jin, T., *et. al.*, Acoustic field characteristics and performance analysis of a looped travelling-wave thermoacoustic refrigerator, *Energy Conversion and Management*, *123* (2016), pp. 243-251.

[24] Swift, G.W., Thermoacoustic Engines, *J. Acoust. Soc. Am*., *84* (1988), pp. 1159-1160

[25] Ueda, Y., *et. al*., Acoustic field in a thermoacoustic Stirling engine having a looped tube and resonator, *Applied Physics Letter*, *81* (2002), pp. 5252-5254.

Paper submitted: 23.04.2023
Paper revised: 18.09.2023
Paper accepted: 27.09.2023